microbial biotechnology

Open Access

Combination of an engineered *Lactococcus lactis* expressing CXCL12 with light-emitting diode yellow light as a treatment for scalded skin in mice

Xiaoxiao Zhao,[1,†] Shengjie Li,[1,†] Jianing Ding,[1] Jing Wei,[1] Puyuan Tian,[1] Hong Wei[2,*] and Tingtao Chen[1,*]

[1]*Institute of Translational Medicine, Nanchang University, Nanchang, Jiangxi, 330031, China.*
[2]*Precision Medicine Institute, The First Affiliated Hospital, Sun Yat-sen University, Guangzhou, Guangdong, 510080, China.*

Summary

Impaired wound closure is an increasingly crucial clinical challenge. Recently, wound healing has shifted towards innovative treatments that exploit nanotechnology, biomaterials, biologics and phototherapy. Here, we constructed an engineered MG1363-pMG36e-mCXCL12 strain with pMG36e plasmid encoding stromal cell-derived factor 1α (named CXCL12) and evaluated the synergistic effects of light-emitting diode (LED) yellow light and MG1363-pMG36e-mCXCL12 on scald wounds in mice. The results indicated that the combined treatment with LED yellow light with mCXCL12 delivering strain accelerated wound closure, tissue remodelling, re-epithelialization and hair follicle regeneration and inhibited over-inflammation oppositely in the central and surrounding wounds by macroscopic, histopathologic and immunohistochemistry parameters. Furthermore, combination therapy increased the epidermal growth factor and Ki67-positive cells and upregulated beta-catenin (β-catenin), cellular-myelocytomatosis (c-Myc), wingless-type MMTV integration site family member 1 (Wnt1), Jagged 1, neurogenic locus notch homolog protein 1 (Notch 1) and hairy and enhancer of split 1 (Hes 1) protein levels of the Wnt and Notch signalling pathways. It also facilitated collagen fibrogenesis and deposition and improved the activities of hydroxyproline, superoxide dismutase and glutathione peroxidase in scalded granulation tissue, in addition to reducing the inflammatory factors interleukin 1 beta (IL-1β) and tumour necrosis factor alpha (TNF-α). The combined treatment effectively reduced skin pathogens *Ralstonia* and *Acinetobacter* to further reduce the risk of infection. Overall, combination of LED yellow light and MG1363-pMG36e-mCXCL12 represents a potential strategy for the treatment of cutaneous wounds.

Introduction

Skin burn is a common form of skin trauma, which refers to the tissue damage caused by high-temperature liquid, steam, hot metal, electric current, laser or chemical substances (Shi *et al*., 2017). According to the World Health Organization (WHO), approximately 300 000 people die from burn injuries each year, which has become the top 15 global disease burdens (Lunawat *et al*., 2016; Lang *et al*., 2019). According to the degree of burn injuries, it can be divided into three degrees: first-degree burns only to the epidermis, second-degree burns only to the dermis and third-degree burns only to the whole cortex (Santos *et al*., 2017).

Current treatment of burn injuries includes drug, physical, radiation, laser and surgical treatment (Hamblin *et al*., 2016; Oh, 2019; Shi *et al*., 2020). However, these methods still have many shortcomings, such as expensive, high side effects, prone to scar hyperplasia and blocking pores (Hamblin *et al*., 2016). Therefore, it is particularly urgent to find a treatment with good curative effects, safety, non-toxic side effects and reasonable price. Wound repair involves the participation of many kinds of cells and cytokines and contains coagulation, inflammation, proliferation and remodelling (Su *et al*., 2019). Studies have found that during the repair of deep second-degree skin burns, the body first undergoes a coagulation reaction to form a protective film that can prevent the invasion of pathogenic microorganisms (Rees *et al*., 2015).

Meanwhile, it also releases many cell growth factors, whose prominent role is to recruit granulocyte and

Received 20 February, 2021; revised 14 June, 2021; accepted 22 June, 2021.
For correspondence. *E-mail chentingtao1984@163.com; Tel./Fax +86 079183827165. **E-mails weih26@mail.sysu.edu.cn; weihong63528@163.com; Tel./Fax +86 02087755766.
[†]Contribute equally to this work.
This study was supported by the National Natural Science Foundation of China (Grant no. 82060638), Academic and technical leaders of major disciplines in Jiangxi Province (Grant no. 20194BCJ22032), and Double thousand plan ofJiangxi Province (high end Talents Project of scientific andtechnological innovation).
Microbial Biotechnology (2021) **14**(5), 2090–2100
doi:10.1111/1751-7915.13885

monocyte cells, fibroblasts into the wound and enhance the repair ability of tissue cells (Thones *et al*., 2019). Neutrophils begin to proliferate in large numbers about 6 h after trauma and reach the peak on the second days (Phillipson and Kubes, 2019). Then, macrophages enter the scalded surface, phagocytize cell fragments and secrete cell growth factors to promote granulation tissue formation. The remodelling phase of wound healing mainly involves reconstructing connective tissue, wound contraction and scar formation (Kim and Nair, 2019).

Recently, more and more clinical studies have shown that probiotics are related to the host's health (Krishnan *et al*., 2016). Probiotics refer to the living bacterial preparation and their metabolites that can improve the host's micro-ecological balance and play a beneficial role in improving the host's health level and health status (Williams, 2010). The metabolites of these bacteria, butyric acid, propionic acid and acetic acid can inhibit the growth and reproduction of pathogenic bacteria, among which *Lactobacillus* and *Lactococcus* are the most widely used strains (Johnson *et al*., 2015). As a kind of food-grade bacteria, *Lactococcus lactis* has been widely studied. It has the characteristics of rapid growth, simple metabolism, no endotoxin production, no spore production, no inclusion body formation, no extracellular protease production and a monolayer membrane that is easy to secrete exogenous proteins, relatively few intracellular and extracellular proteins, and easy to purify, and often used as a delivery vector of therapeutic proteins, DNA and vaccine antigens (Cano-Garrido *et al*., 2014; Geldart *et al*., 2015).

Various cytokines are involved in the skin wound-healing process, including pro-inflammatory factors interleukin 1 beta (IL-1β) and tumour necrosis factor alpha (TNF-α), chemokines, epidermal growth factor (EGF) and transforming growth factor (TGF). The chemokine CXCL12 (stromal cell-derived factor 1α) is expressed rapidly in response to tissue injury and effectively enhances wound healing and reduces tissue scar formation by recruiting and proliferating macrophages (Rabbany *et al*., 2010). Burn injuries will destroy the skin's barrier function, increase the risk of wound infection and make it easy to have systemic inflammatory reaction, sepsis and multiple organ dysfunction syndrome (Grice and Segre, 2011; Fan *et al*., 2019). Interestingly, *L. reuteri* has been used as a carrier to load chemokine CXCL12 to treat wounds, and this recombinant bacteria accelerated wound healing by stimulating the proliferation of keratinocytes and improving the bioavailability of CXCL12 under acidic conditions (Vagesjo *et al*., 2018).

Moreover, with the rise of light-emitting diode (LED) spectroscopy in the beauty industry, the use of light therapy to assist wound treatment has become a hot topic in recent years (Rathnakar *et al*., 2016; Chang *et al*., 2018). Previous studies have shown that LED with different wavelengths plays a different role in medicine. For example, red light of the spectrum 630–770 nm can effectively relieve wound pain and promote wound healing (Li *et al*., 2016; Rocha Mota *et al*., 2018), whereas violet and blue light peaking at 405–470 nm can sterilize wounds (Dos Santos *et al*., 2018). Yellow light at 570–600 nm can stimulate collagen synthesis to tighten the skin (Jagdeo *et al*., 2018; Oh and Jeong, 2019). However, there are few studies on yellow light-assisted wound healing.

In the present study, engineered MG1363-pMG36e-mCXCL12 was constructed, and a skin scald animal model was developed to study the potential of the combination of MG1363-pMG36e-mCXCL12 and light-therapy LED yellow light as a skin scald drug, via monitoring the effects on wound healing, inflammatory factors and skin microbiota.

Results

Construction and verification of the engineered MG1363-pMG36e-mCXCL12

The codon-optimized murine CXCL12 (NM_021704.3) was inserted into vector pMG36e with a signal peptide sequence (amino acid sequence: MNAKVVVVLVLVLTALCLSDG) and then electrically transformed into *L. lactis* subsp cremoris (strain MG1363) to produce the MG1363-pMG36e-mCXCL12 strain. The ELISA result indicated that about 94 pg ml^{-1} mCXCL12 was produced by MG1363-pMG36e-mCXCL12, and 100% and 83% of the plasmids were still existed in the engineered bacteria after 7 day and 30 days, respectively (Y. Kong, X. Zhao, Z. Liu, and T. Chen, unpublished data).

Gross examination and measurements of wound size

In this experiment, scalded mice were randomly divided into groups C, L, LC, Y, LY and LCY, with 16 mice in each group. Changes in the wounds' overall appearance were observed on days 0, 2, 6, 10, 14 and 18 after scalding. Four mice were killed in each group on days 3, 9 and 15, and skin tissue was taken for experimental analysis (Fig. 1A). The results illustrated that the LCY group had the best treatment effect during the healing cycle (Fig. 1B), with a healing rate of 99.11% on the 18th day, followed by the LC group (92.99%), the LY group (86.35%) and the L group (77.35%) (Fig. 1C). No significant difference in the wound-healing rate was observed between the C and Y groups (Fig. 1B and C), indicating that LED yellow light alone has little effect on wound healing, whereas its combination with MG1363-pMG36e-mCXCL2 accelerated the wound-healing process in the LCY group.

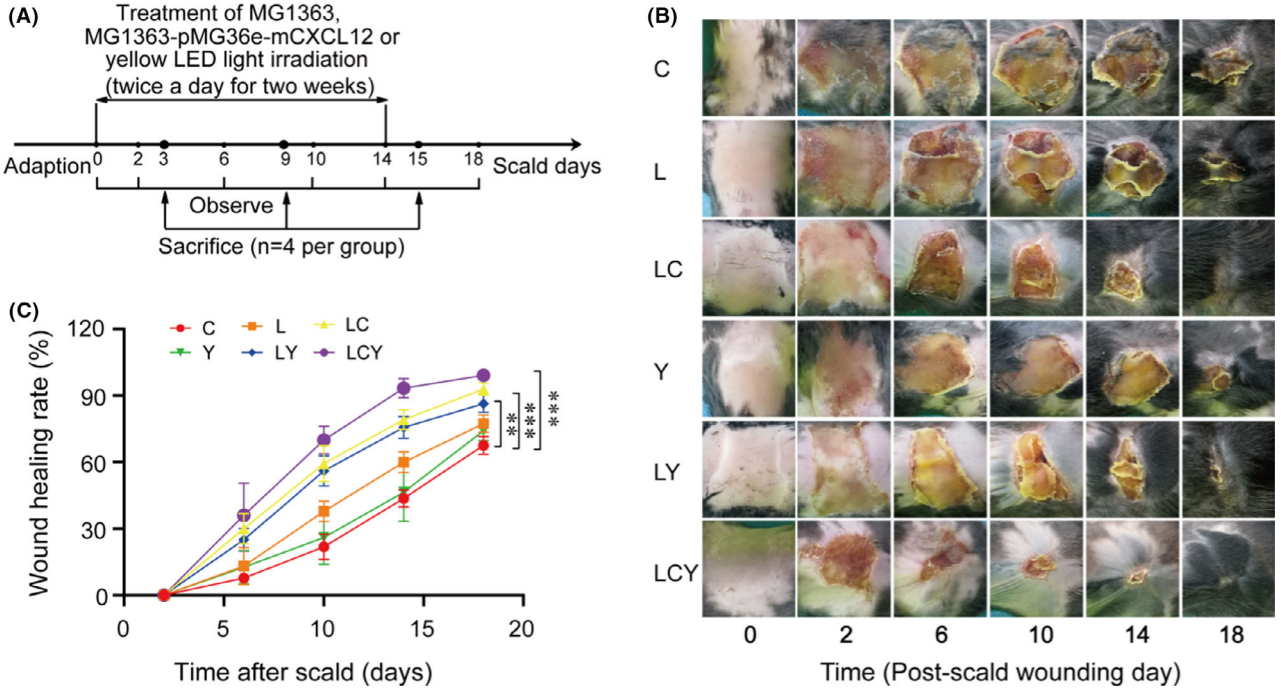

Fig. 1. Combination of MG1363-pMG36e-mCXCL12 and LED yellow light promotes wound closure.
A. Experimental scheme for scald wound mice. The scald mice were randomly divided into six groups ($n = 16$ per groups); after scalding, the mice were treated immediately for 14 days. Scald areas were evaluated on days 0, 2, 6, 10, 14 and 18. Then, the mice were sacrificed on the 3rd, 9th and 15th days.
B. Gross appearance of scald wound.
C. Wound-healing rate (n = 4 per group; two-way ANOVA with Bonferroni post-test, $^{**}P < 0.001$, $^{***}P < 0.0005$). The C group was treated with saline, the L group with MG1363, the LC group with MG1363-pMG36e-mCXCL12, the Y group with LED yellow light irradiation, the LY group with MG1363+LED yellow light irradiation and the LCY group with MG1363-pMG36e-mCXCL12+LED yellow light irradiation.

MG1363-pMG36e-mCXCL12 and LED yellow light synergistically inhibit inflammatory responses in scalded skin

To further observe the effects of MG1363-pMG36e-mCXCL12 and LED yellow light on the regeneration of wound epidermis and dermis, skins of animals in each group were sampled on days 3, 9 and 15. Epidermal damage and a large number of inflammatory cells were found in each group on the 3rd day, and numerous inflammatory cells were also identified in the C, Y, L and LY groups on the 9th day (Fig. 2A). The inflammatory cells were reduced, and the dermis was gradually repaired in the LCY and LC groups, especially for the LCY group, in which connective tissue was well reconstituted and some keratinous epithelium and dermal cells were arranged regularly on the 15th day (Fig. 2A).

We also detected the expression of IL-1β and TNF-α, since the damaged tissue underwent a slow-onset persistent inflammatory response, focusing on the release of pro-inflammatory factors IL-1β and TNF-α after skin damage. The levels of IL-1β and TNF-α were dramatically increased. However, treatment using MG1363-pMG36e-mCXCL12 greatly mediated the organismal response of the host to the inflammatory response, as MG1363-pMG36e-mCXCL12 could restore the IL-1β and TNF-α to a normal level with the assistance of LED yellow light in the LCY group (Fig. 2B and C).

MG1363-pMG36e-mCXCL12 and LED yellow light synergistically accelerate re-epithelialization of scalded skin

Cell proliferation and differentiation play a vital role in the proliferation stage of wound healing, and therefore, we evaluated the effects of the MG1363-pMG36e-mCXCL12 on the regeneration of wound epidermis and the growth of granulation tissue sequentially and of LED yellow light synergistically. Compared with the N group, the immunohistochemistry results showed that skin injury decreased the numbers of EGF- and Ki67-positive cells, and the treatments increased the number of EGF- and Ki67-positive cells on the wound surface of the mice, particular in the LC and LCY groups (Fig. 3A). Furthermore, compared with the standard group, the protein levels of beta-catenin (β-catenin), cellular-myelocytomatosis (c-Myc) and wingless-type MMTV integration site family member 1 (Wnt1) in deep second-degree scalded mice

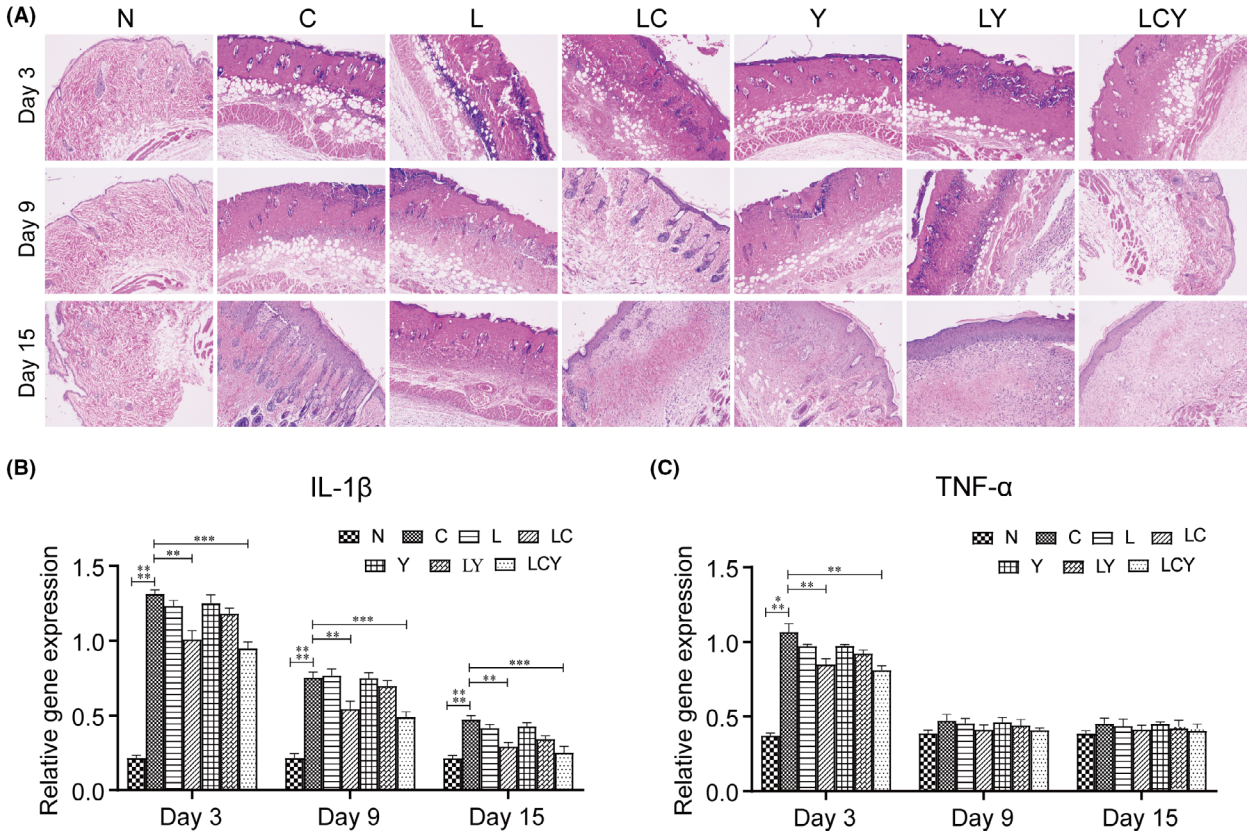

Fig. 2. Effect of engineered combined with light on inflammation in the wound-healing process of scalded mice.
A. Stained with H&E stain of the wounds in the C, L, LC, Y, LY and LCY groups at 3, 9 and 15 days post-scald (n = 4 per group). Magnification: ×100.
B. The gene levels of IL-1β and (C) TNF-α in skin tissues of experimentally scalded mice (n = 4 per group; one-way ANOVA Kruskal–Wallis test, $^{*}P < 0.05$, $^{**}P < 0.001$). The N group was not scalded, C group treated with saline, L group treated with MG1363, LC group treated with MG1363-pMG36e-mCXCL12, Y group treated with LED yellow light irradiation, LY group treated with MG1363+LED yellow light irradiation and LCY group treated with MG1363-pMG36e-mCXCL12+LED yellow light irradiation.

were significantly decreased, but the combination of MG1363-pMG36e-mCXCL12 and LED yellow light synergistically reversed the status of critical proteins in Wnt pathways in the LCY group (Fig. 3B). Similarly, it also greatly enhanced the protein levels of Jagged 1, neurogenic locus notch homolog protein 1 (Notch 1) and hairy and enhancer of split 1 (Hes 1) in the Notch signalling pathways (Fig. 3C).

MG1363-pMG36e-mCXCL12 and LED yellow light synergistically increase collagen deposition and inhibition of lipid peroxidation

In the process of deep scald wound repair, collagen deposition and repair are the prominent manifestations. Therefore, we performed Masson staining on the skin of mice on the 9th day. As shown in Fig. 4A, the skin in the C, L and Y groups had fewer stained collagen fibres than normal skin, which were sparsely and unorderly arranged. In contrast, the content of stained collagen increased significantly in the LY, LC and LCY groups; the collagen fibres in the skin were orderly arranged with a more uniform density in the LCY group.

We further compared the protein levels of hydroxyproline (HyP), superoxide dismutase (SOD) and glutathione peroxidase (GSH-Px) among all groups, and our results indicated that skin wounding significantly reduced the yields of HyP, SOD and GSH-Px, whereas MG1363-pMG36e-mCXCL12 could reverse this trend; the combination of MG1363-pMG36e-mCXCL12 and LED yellow light showed the best effect (Fig. 4B–D).

Synergistic effects of MG1363-pMG36e-mCXCL12 and LED yellow light on skin microbiota

The skin microbiome maintains the skin barrier function, regulating inflammation and stimulates the wound-healing response. Therefore, we used 16S rRNA high-throughput sequencing to explore the effects of MG1363-pMG36e-mCXCL12 and yellow light treatment

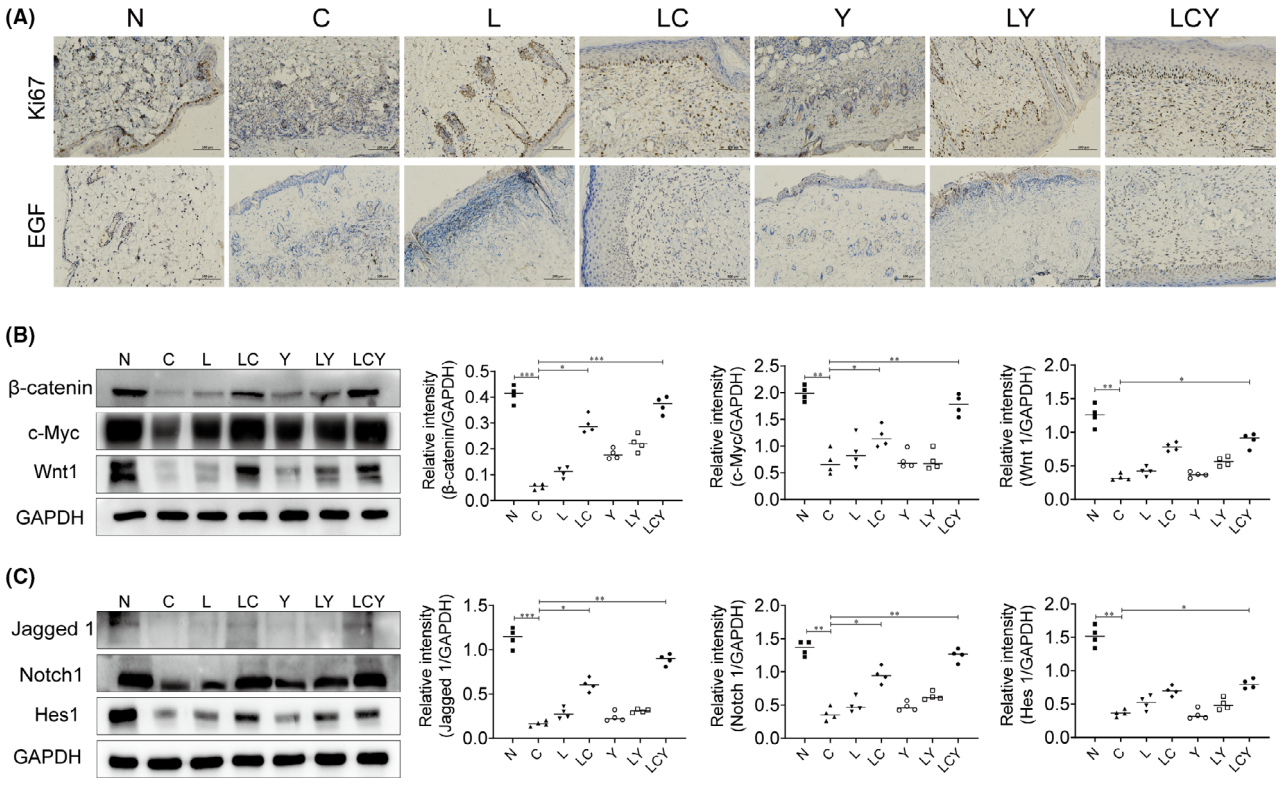

Fig. 3. Re-epithelialization of wound skin after treatment with engineered strains combined with light.
A. Skin wounds were IHC-stained for Ki67^{+} and EGF populations of the wounds in the C, L, LC, Y, LY and LCY groups on the 9 day post-scald ($n = 4$ per group). The bar corresponds to 100 μm.
B. C. The relative protein expressions of β-catenin, c-Myc, Wnt1, Jagged 1, Notch 1 and Hes 1 compared with GAPDH were analysed by Western blot of the wounds in the C, L, LC, Y, LY and LCY groups on the 9 day post-scald and normal mice ($n = 4$ per group; one-way ANOVA Kruskal–Wallis test, $^{*}P < 0.05$, $^{**}P < 0.001$, $^{***}P < 0.0005$).

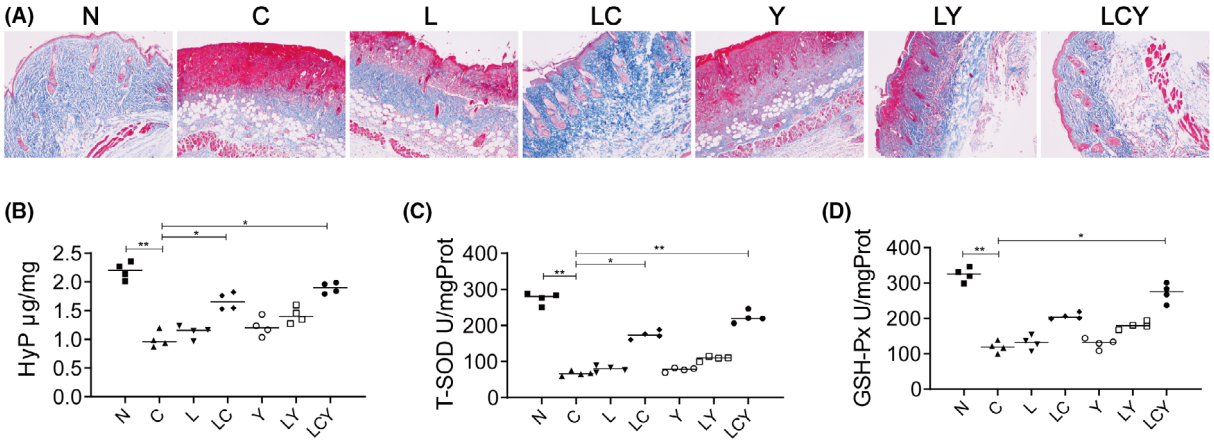

Fig. 4. Effect of engineered strains combined with light on collagen generation in the wound-healing process of scalded mice.
A. Stained with Masson stain in the C, L, LC, Y, LY and LCY groups on the 9th day post-scald ($n = 4$ per group). Magnification: 100. Levels of (B) hydroxyproline (C) superoxide dismutase and (D) glutathione peroxidase in the scald wounds. Scald wounds were collected from each group on day 9 after injury ($n = 4$ per group, one-way ANOVA Kruskal–Wallis test, $^{*}P < 0.05$, $^{**}P < 0.001$).

on the microbial composition of burns and scalds. Compared with the standard group, scalding increased the Shannon index ($P < 0.05$), and the groups LC and LCY were conductive to restore the bacterial balance to normal composition (Fig. 5A). Subsequently, we investigated the two most common phyla; compared with normal mice, scalding reduced the abundance of Proteobacteria (99.65 vs. 96.45%) and increased the

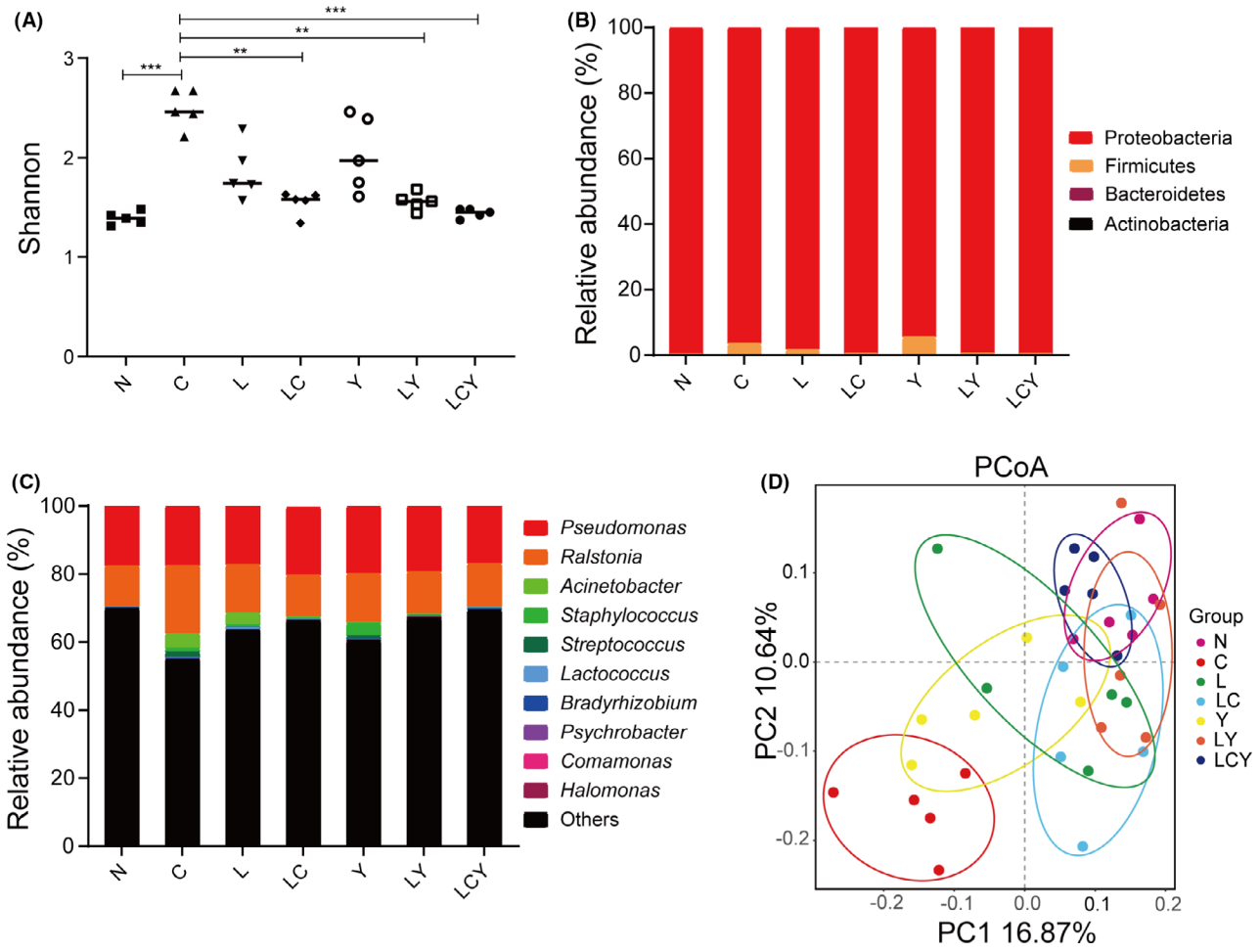

Fig. 5. Effects of engineered strains combined with light on scald skin microbiota.
A. Shannon diversity.
B. Microbial composition at the phylum level.
C. Microbial composition at the genus level.
D. PCoA of β diversity index. Scald skin microbiota were collected from each group on day 10 after injury ($n = 5$ per group; one-way ANOVA Kruskal–Wallis test, $^{*}P < 0.05$, $^{**}P < 0.001$).

division of Firmicutes (0.23% vs. 3.47%) (Fig. 5B). At the genus level, compared with the standard group, mice in the scalding group showed an increased relative abundance of *Ralstonia* (12.03% vs. 19.89%) and *Achinetobacter* (0.12% vs. 4.37%), and treatment with LC and LCY effectively reversed this trend (Fig. 5C). Moreover, abundance of *Lactococcus* increased in groups L, LC, LY and LCY. Based on the results of the PCoA, all samples in group C deviated significantly from those in group N, whereas 3/5 samples in group LC and 1/5 samples in group LCY were far from those from group N (Fig. 5D). These results suggest that the microbial composition was changed after scalds, but the use of MG1363-pMG36e-mCXCL2L in both the LC and LCY groups restored a new microbial balance, making it closer to normal mouse microbiome.

Discussion

Scalding is a common accidental injury in daily life, usually caused by contacting scalding liquids or metals (Evers *et al.*, 2010). If the scalded wound is not treated in time, it is likely to cause skin necrosis and leave sequelae (Palmieri and Romanowski, 2017). Ointment, cream, biological and abiotic dressings, as well as antibiotics, are recommended for 1st-, 2nd- and 3rd-degree burns; however, the abuse of drugs increases the risk of antibiotic resistance and fungal infections, even slowing wound healing and increasing the depth of the burn (Bielefeld *et al.*, 2013; Garg and Singh, 2019). Here, we developed a technology to treat scalded skin in a mice model using engineered *L. lactic* MG1363 with a plasmid encoding mCXCL12 combined with yellow light, which

significantly accelerated the healing of skin wounds and improved the speed of wound contraction, epithelial formation and maturation.

The inflammatory response is a comprehensive manifestation of the interaction of several factors such as pro-inflammatory and anti-inflammatory ones after tissue injury and plays an important role in the initial phase of wound healing (Nishio *et al*., 2008; Carter *et al*., 2014). During healing, the released IL-1β and TNF-α initiate inflammation (Pasparakis, 2009). In this study, we observed that the combined treatment of MG1363-pMG36e-mCXCL12 and yellow light decreased the number of inflammatory cells, accelerated reepithelization and wound closure (Fig. 2A), reduced excessive inflammation and down-regulated the mRNA levels of IL-1β and TNF-α (Fig. 2B and C), suggesting that this technology could alleviate scald symptoms by inhibiting the pro-inflammatory response.

Cell proliferation and differentiation play a significant regulatory role in the process of scald repair, and $Ki67^+$ is one of the primary markers of cell proliferation (Graefe *et al*., 2019). After skin injury, platelet aggregation will occur locally, and subsequently, the aggregated platelets and damaged keratinocytes release EGF, which promotes the proliferation, differentiation and maturation of keratinocytes, and further acts on dermal fibroblasts to encourage secretion collagen (Eming *et al*., 2014). We observed an increase in wound epidermal growth factor and $Ki67^+$ cells in the LCY treatment group (Fig. 3A). Furthermore, the protein expression levels of β-catenin, c-Myc, Wnt1, Jagged 1, Notch 1 and Hes 1 in the Wnt and Notch signalling pathways were also upregulated (Fig. 3B and C). These findings indicate that our technology promotes skin tissue proliferation and epidermal differentiation by increasing EGF levels and upregulating the Wnt and Notch signalling pathways (Barrientos *et al*., 2008).

During wound healing, connective tissue mainly consists of fibroblasts and collagen, and the collagen content has an immediate impact on the wound repair process (Kulshrestha *et al*., 2019). We observed that collagen in scalded skin was evenly distributed in the LCY group (Fig. 4A). The increase in the level of HyP (a precursor amino acid of collagen synthesis and the HyP content of granulation tissue that represents the collagen level) in the wound (Fig. 4B) further indicated that LCY treatment could regulate the production of collagen and increase the level of collagen fibres and collagen in the skin, which was beneficial to wound repair (Liang *et al*., 2019). In addition, higher levels of SOD and GSH-Px were observed in the LCY group, indicating that the combination of MG1363-pMG36e-mCXCL12 and yellow light could upregulate the activity of the oxidative defence system in scalded tissues and protect the body from oxidative stress damage, thereby reducing infection levels (Parihar *et al*., 2008). We studied the symbiotic skin bacteria in animal skin, which are the basis for maintaining the skin barrier and preventing infections by pathogenic bacteria and other microorganisms (Zhou *et al*., 2010). There is considerable evidence that skin surface microorganisms can affect wound healing (Thomas-Virnig and Allen-Hoffmann, 2012; Yoon *et al*., 2018). Our results indicated that scalds change the microbial diversity on the skin, and LCY treatment helped to restore the new dynamic balance of the microbiota (Fig. 4), effectively inhibiting the relative abundances of *Ralstonia* and *Acinetobacte*r, which could increase the risk of wound infection, leading to non-healing wounds or other complications (Ryan and Adley, 2014; Wong *et al*., 2017).

In the present study, we constructed the engineered bacteria MG1363-pMG36e-mCXCL12. They could effectively accelerate wound healing via increased antioxidant activity, as evidenced by the increase in SOD and GSH-Px levels, enhance cell proliferation and differentiation through the Wnt and Notch signalling pathways and accelerate collagen synthesis through increased HyP expression, they also restored the disturbed microbiota, with the assistance of LED yellow light. Although our study is limited by the small number of mice, this approach provides an efficient novel alternative to treat cutaneous wounds.

Experimental procedures

Strains and plasmids

According to the host bacteria *L. lactis*, the DNA sequence of murine CXCL12 (NM_021704.3) was codon-optimized, and we added a signal peptide sequence at the front of the sequence. All gene fragment sequences were synthesized at Sangon Biotechnology Co., Ltd., Shanghai, China. This fragment was inserted into vector pMG36e (prokaryotic expression vector), using XbaI and Pst I restriction enzyme to produce plasmid pMG36e-mCXCL12. Subsequently, *L. lactis* subsp *cremoris* (strain MG1363) was electrically transformed with the plasmid pMG36e-mCXCL12 to produce the MG1363-pMG36e-mCXCL12 strain on the GM17 plate (Hope Bio, Qingdao, China, M17 medium containing 5% glucose) with erythromycin (100 μg ml^{-1}). Then, we used a live count to test plasmid stability over time without antibiotic culture. The mCXCL12 capability via direct expression was verified using the ELISA Kit for the stromal cell-derived factor 1 (Cloud-Clone, Wuhan, China).

Bacterial culture

Strains *L. lactis* MG1363 and MG1363-pMG36e-mCXCL12 grown overnight in GM17 medium. The

overnight culture was reinoculated at a 1:100 dilution in fresh medium and grown to $OD_{600} = 0.5$. Bacteria were centrifuged at 3000 rpm for 6 min and washed three times with sterile saline. Subsequently, there were diluted with sterile saline to 10^9 CFU ml^{-1}.

Animal model

We purchased 112 6- to 8-week-old male C57BL/6 mice from Si Lake King of Experimental Animal Co., Ltd. (Changsha, Hunan, China). Mice were housed individually in cages, allowed free access to a standard diet and water and were weighed in the Laboratory Animal Center of Nanchang University. Ninety-six mice were randomly selected for scalding. The remaining mice were assigned to the normal control group (*N*).

Twenty-four hours prior to scalding, the hair on the scalp was removed with electric hair clippers and treated with depilatory cream. The second-degree scald wound mice model was built with hot water (90°C for 10 s) on the dorsal surface, and the size of the wound was approximately 2.25 cm^2 (1.5 × 1.5 cm). The mice were immediately intraperitoneally injected with 1 ml kg^{-1} sterile saline to prevent shock (Zhang *et al*., 2019).

The model mice were divided into six groups, with 16 mice per group at random. The C group was treated with saline, the L group with 2×10^7 CFU of *L. lactis* MG1363, the LC group with 2×10^7 CFU of *L. lactis* MG1363-pMG36e-mCXCL12, the Y group with LED yellow light, the LY group with a combination therapy of 2×10^7 CFU MG1363 strain and LED yellow light, the LCY group with a combination therapy of 2×10^7 CFU of MG1363-pMG36e-mCXCL12 strain and LED yellow light. We dabbed 20 μL of 10^9 CFU ml^{-1} of the corresponding strain on the wound surface, using sterile swabs. Light treatment consisted of light-emitting diode (LED) yellow light at a distance of 20 cm from the wound for 2 h. All treatments were applied twice a day, morning and evening, for 2 weeks. On days 3, 9 and 15, four mice per group were sacrificed, and the scalded skin was excised. Part of the skin samples were used for histological examination, and the remaining tissue samples were stored at −80°C. The study was approved by the Ethical Committee of the Nanchang Royo Biotech Co. Ltd. (Nanchang City, China), and all experiments were conducted in conformity to the approved guidelines (ID number RYE2019043001).

Macroscopic analysis of scald wound

The scald areas were photographed on days 0, 2, 6, 10, 14 and 18 following the scald injury and analysed using Image-Pro Plus 6.0. The wound-healing rate (x) was calculated based on the equation in the main text, where A = the original wound area and A_t = the detection area.

$$x = \frac{A - A_t}{A_t} \times 100\%.$$

Histological examination

Scald skin tissue samples were fixed in neutral buffered formalin and embedded in paraffin, cut into 5-μm-thick sections and stained with haematoxylin and eosin and Masson-Goldner trichrome staining to visualize morphological features and fibrosis. For immunohistochemistry (IHC) staining, primary antibodies anti-Ki67 (1:200; Servicebio, Wuhan, China; Cat# GB111499) and anti-EGF (1:200; Bioss, Beijing, China; Cat# bs-2009R) were used.

Real-time quantitative PCR

According to the manufacture's protocol, total RNA was extra**c**ted from the skin tissue using TRIzol Reagent (Invitrogen, Carlsbad, CA, USA; Cat# 15596026). All reagents for RT-qPCR were purchased from Takara Bio (Otsu, Japan). All procedures were strictly performed according to the manufacturers' protocol. The RT-qPCRs were performed using an ABI 7500 fast real-time PCR system (Applied Biosystems, Foster City, CA, USA). The amplification conditions were 95°C for 30 s, followed by 40 cycles of degeneration at 95°C for 5 s and 60°C for 34 s. The relative expression levels were calculated using the $2^{-\Delta\Delta Ct}$ method.

We used the following primers: primers 5'-GTGTCTTT CCCGTGGACCTTC-3' and 5'-TCATCTCGGAGCCT GTAGTGC-3' for IL-1β, primers 5'-GTGGAACTGGC AGAAGAGGCA-3' and 5'-AGAGGGAGGCCATTTGGGA AC-3' for TNF-α, and primers 5'-CTCGTGGAGTCTAC TGGTGT-3' and 5'-GTCATCATACTTGGCAGGTT-3' for GAPDH.

Western blot analysis

Skin tissues were lysed in RIPA lysis buffer (Solarbio, Beijing, China; Cat# R0010) and centrifuged at 13 000 rpm for 10 min at 4°C. Protein quantitation was conducted using the Pierce™ Rapid Gold BCA Protein Assay Kit (Thermo Fisher, Waltham, MA, USA; Cat# A53226). Subsequently, 40 μg of proteins was separated by sodium dodecyl sulphate-polyacrylamide gel electrophoresis (SDS-PAGE) on 10–15% gels and electrotransferred to polyvinylidene difluoride membranes (Millipore, Bedford, MA, USA; Cat# IPVH00010). After blocking with 5% skim milk at room temperature for 1 hour (h), the membranes were incubated with specific primary antibodies against Wnt 1 (1:1000; ProteinTech,

Sanying Biotechnology, Wuhan, China; Cat# 27935-1-AP), Notch 1 (1:1000; ProteinTech, Sanying Biotechnology; 20687-1-AP), Jagged 1 (1:1000; Bioss; Cat# bs-1448R), c-Myc (1:5000, sc-40; Santa Cruz Biotechnology, USA; Cat# sc-40), β-catenin (1:1000; Cell Signaling Technology, Beverly, MA, USA; Cat# 3700S), Hes 1 (1:1000; Cell Signaling Technology; Cat# 11988S) and GAPDH (1:2000; Cell Signaling Technology; Cat# 5174S) at 4°C overnight. After three washes, the membranes were incubated with goat anti-rabbit (1:5,000; ProteinTech, Sanying Biotechnology; Cat# SA00001-2) or goat anti-mouse (1:5,000; Bioss; Cat# bs-40296G-HRP) for 1 h at room temperature. Finally, the specific proteins were detected using the Pierce™ ECL Western Blotting Substrate (Thermo Fisher; Cat# 32209).

Activity analysis of hydroxyproline, superoxide dismutase and glutathione peroxidase

The 10% scald skin tissue homogenate was prepared with 0.86% saline and centrifuged at 3000 rpm for 10 min at 4°C. HyP, SOD and GSH-Px activities were measured using commercial kits according to the manufacturer's instructions.

High-throughput sequencing analyses

Microorganisms from the skin wound were collected with sterile swabs on the 10^{th} day ($n = 5$, per group). The skin microbial DNA was extracted according to the operating instructions of the DNA extraction kit (Tiangen, Beijing, China; Cat# DP302-02). The concentration and quality of extracted genomic DNA were quantified using a NanoDrop spectrophotometer.

The composition and diversity of the microbiota were analysed by 16S rRNA high-throughput sequencing; 16S rRNA genes of V4 regions were amplified using 515F: 5'-GTGCCAGCMGCCGCGGTAA-3' and 806R: 5'-GGACTACHVGGGTWTCTAAT-3' primers with barcodes. We used the Illumina MiSeq platform to pair-end DNA fragments in the community and the QIIME software (v. 1.8.0, http://qiime.org/) to analyse the original sequencing data, carrying out screening, processing and quality control (GenBank accession number PRJNA727743) (Caporaso *et al*., 2010). We merged the operational taxonomic unit (OTU) division of the sequences obtained above according to the sequence similarity of 97% and selected the most abundant sequence in each OTU as the representative sequence of the OTU (Edgar, 2010). Subsequently, we analysed the alpha diversity (Chao, ACE, Shannon and Simpson diversity index) and beta diversity (Principal coordinates analysis, principal co-ordinates analysis (PCoA) and Nonmetric Multidimensional Scaling (NMDS)) through the QIIME software (v. 1.8.0) (Ramette, 2007). The QIIME software was used to obtain the composition and abundance distribution table of each sample at the five classification levels of phylum, class, order, family and genus; the results were presented through stacked histograms.

Data analysis

Results were treated as biological replicates. Data normality was not separately assessed. Grubbs' outlier test indicated that no outlier was found. The Prism software version 8.0 (GraphPad Software, San Diego, CA, USA; RRID: SCR_004812) was used for statistical analysis. Data are presented as mean ± standard deviation (SD). Statistical significance was analysed using one-way analysis of variance (ANOVA) followed by the Kruskal–Wallis test. Statistical significance was set at $P < 0.05$.

Acknowledgements

We sincerely thank all the subjects and our colleagues who contributed to the study.

Funding Information

This study was supported by the National Natural Science Foundation of China (Grant no. 82060638), Academic and technical leaders of major disciplines in Jiangxi Province (Grant no. 20194BCJ22032) and Double thousand plan of Jiangxi Province (High-End Talents Project of scientific and technological innovation).

Conflicts of interest

All authors declare that they have no conflicts of interest.

Ethical approval

All applicable international, national and/or institutional guidelines for the care and use of animals were followed.

Authors' contributions

TC and HW designed the experiment; XZ, TC and SL analysed the data and wrote the manuscript. All authors discussed the results and commented on the manuscript.

References

Barrientos, S., Stojadinovic, O., Golinko, M.S., Brem, H., and Tomic-Canic, M. (2008) Growth factors and cytokines in wound healing. *Wound Repair Regen* **16:** 585–601.

Bielefeld, K.A., Amini-Nik, S., and Alman, B.A. (2013) Cutaneous wound healing: recruiting developmental pathways for regeneration. *Cell Mol Life Sci* **70:** 2059–2081.

Cano-Garrido, O., Rueda, F.L., Sànchez-García, L., Ruiz-Á vila, L., Bosser, R., Villaverde, A., and García-Fruitós, E. (2014) Expanding the recombinant protein quality in *Lactococcus lactis*. *Microb Cell Fact* **13:** 167–173.

Caporaso, J.G., Kuczynski, J., Stombaugh, J., Bittinger, K., Bushman, F.D., Costello, E.K., *et al*. (2010) QIIME allows analysis of high-throughput community sequencing data. *Nat Methods* **7:** 335–336.

Carter, D., Warsen, A., Mandell, K., Cuschieri, J., Maier, R.V., and Arbabi, S. (2014) Delayed topical p38 MAPK inhibition attenuates full-thickness burn wound inflammatory signaling. *J Burn Care Res* **35:** 83–92.

Chang, M.H., Hsiao, Y.P., Hsu, C.Y., and Lai, P.S. (2018) Photo-crosslinked polymeric matrix with antimicrobial functions for excisional wound healing in mice. *Nanomaterials (Basel)* **8:** 791.

Dos Santos, M.S.C., Gouvêa, A.L., de Moura, L.D., Paterno, L.G., de Souza, P.E.N., Bastos, A.P., *et al*. (2018) Nanographene oxide-methylene blue as phototherapies platform for breast tumor ablation and metastasis prevention in a syngeneic orthotopic murine model. *J Nanobiotechnol* **16:** 9–26.

Edgar, R.C. (2010) Search and clustering orders of magnitude faster than BLAST. *Bioinformatics* **26:** 2460–2641.

Eming, S.A., Martin, P., and Tomic-Canic, M. (2014) Wound repair and regeneration: mechanisms, signaling, and translation. *Sci Transl Med* **6:** 265sr6.

Evers, L.H., Bhavsar, D., and Mailander, P. (2010) The biology of burn injury. *Exp Dermatol* **19:** 777–783.

Fan, Y., Wu, W., Lei, Y.u., Gaucher, C., Pei, S., Zhang, J., and Xia, X. (2019) Edaravone-loaded alginate-based nanocomposite hydrogel accelerated chronic wound healing in diabetic mice. *Marine Drugs* **17:** 285.

Garg, P.K., and Singh, V.P. (2019) Organ failure due to systemic injury in acute pancreatitis. *Gastroenterology* **156:** 2008–2023.

Geldart, K., Borrero, J., and Kaznessis, Y.N. (2015) Chloride-inducible expression vector for delivery of antimicrobial peptides targeting antibiotic-resistant *Enterococcus faecium*. *Appl Environ Microbiol* **81:** 3889–3897.

Graefe, C., Eichhorn, L., Wurst, P., Kleiner, J., Heine, A., Panetas, I., *et al*. (2019) Optimized Ki-67 staining in murine cells: a tool to determine cell proliferation. *Mol Biol Rep* **46:** 4631–4643.

Grice, E.A., and Segre, J.A. (2011) The skin microbiome. *Nat Rev Microbiol* **9:** 244–253.

Hamblin, M., Keshri, G.K., Gupta, A., Yadav, A., Sharma, S.K., and Singh, S.B. (2016) Photobiomodulation with pulsed and continuous wave near-infrared laser (810 nm, Al-Ga-As) augments dermal wound healing in immunosuppressed Rats. *PLoS One* **11:** e0166705.

Jagdeo, J., Austin, E., Mamalis, A., Wong, C., Ho, D., and Siegel, D.M. (2018) Light-emitting diodes in dermatology: a systematic review of randomized controlled trials. *Lasers Surg Med* **50:** 613–628.

Johnson, L.P., Walton, G.E., Psichas, A., Frost, G.S., Gibson, G.R., and Barraclough, T.G. (2015) Prebiotics modulate the effects of antibiotics on gut microbial diversity and functioning in vitro. *Nutrients* **7:** 4480–4497.

Kim, S.Y., and Nair, M.G. (2019) Macrophages in wound healing: activation and plasticity. *Immunol Cell Biol* **97:** 258–267.

Krishnan, M., Penrose, H.M., Shah, N.N., Marchelletta, R.R., and McCole, D.F. (2016) VSL#3 probiotic stimulates T-cell protein tyrosine phosphatase-mediated recovery of IFN-gamma-induced intestinal epithelial barrier defects. *Inflamm Bowel Dis* **22:** 2811–2823.

Kulshrestha, S., Chawla, R., Alam, M.T., Adhikari, J.S., and Basu, M. (2019) Efficacy and dermal toxicity analysis of Sildenafil citrate based topical hydrogel formulation against traumatic wounds. *Biomed Pharmacother* **112:** 108571.

Lang, T.C., Zhao, R., Kim, A., Wijewardena, A., Vandervord, J., Xue, M., and Jackson, C.J. (2019) A critical update of the assessment and acute management of patients with severe burns. *Adv Wound Care (New Rochelle)* **8:** 607–633.

Li, Y., Zhang, J., Xu, Y., Han, Y., Jiang, B., Huang, L., *et al*. (2016) The histopathological investigation of red and blue light emitting diode on treating skin wounds in japanese big-ear white rabbit. *PLoS One* **11:** e0157898.

Liang, Y., Zhao, X., Hu, T., Chen, B., Yin, Z., Ma, P.X., and Guo, B. (2019) Adhesive hemostatic conducting injectable composite hydrogels with sustained drug release and photothermal antibacterial activity to promote full-thickness skin regeneration during wound healing. *Small* **15:** 1900046.

Lunawat, A., Vashistha, R., Patel, V., Chhabra, R., and Kolla, V. (2016) Predicting mortality in burns: a new scoring system. *Int Surg J* **3:** 271–276.

Nishio, N., Okawa, Y., Sakurai, H., and Isobe, K. (2008) Neutrophil depletion delays wound repair in aged mice. *Age (Dordr)* **30:** 11–19.

Oh, P.S., and Jeong, H.J. (2019) Therapeutic application of light emitting diode: photo-oncomic approach. *J Photochem Photobiol B* **192:** 1–7.

Oh, S.J. (2019) Simultaneous two-layer harvesting of scalp split-thickness skin and dermal grafts for acute burns and postburn scar deformities. *Arch Plast Surg*. **46:** 558–565.

Palmieri, T.L., and Romanowski, K.S. (2017) Pediatric burn resuscitation: past, present, and future. *Burns Trauma* **5:** 26.

Parihar, A., Parihar, M.S., Milner, S., and Bhat, S. (2008) Oxidative stress and anti-oxidative mobilization in burn injury. *Burns* **34:** 6–17.

Pasparakis, M. (2009) Regulation of tissue homeostasis by NF-kappaB signalling: implications for inflammatory diseases. *Nat Rev Immunol* **9:** 778–788.

Phillipson, M., and Kubes, P. (2019) The healing power of neutrophils. *Trends Immunol* **40:** 635–647.

Rabbany, S.Y., Pastore, J., Yamamoto, M., Miller, T., Rafii, S., Aras, R., and Penn, M. (2010) Continuous delivery of stromal cell-derived factor-1 from alginate scaffolds accelerates wound healing. *Cell Transplant* **19:** 399–408.

Ramette, A. (2007) Multivariate analyses in microbial ecology. *FEMS Microbiol Ecol* **62:** 142–160.

Rathnakar, B., Rao, B.S.S., Prabhu, V., Chandra, S., Rai, S., Rao, A.C.K., *et al*. (2016) Photo-biomodulatory response of low-power laser irradiation on burn tissue repair in mice. *Lasers Med Sci* **31:** 1741–1750.

Rees, P.A., Greaves, N.S., Baguneid, M., and Bayat, A. (2015) Chemokines in wound healing and as potential therapeutic targets for reducing cutaneous scarring. *Adv Wound Care (New Rochelle)* **4:** 687–703.

Rocha Mota, L., Motta, L.J., Duarte, I.D.S., Horliana, A., Silva, D., and Pavani, C. (2018) Efficacy of phototherapy to treat facial ageing when using a red versus an amber LED: a protocol for a randomised controlled trial. *BMJ Open* **8:** e021419.

Ryan, M.P., and Adley, C.C. (2014) Ralstonia spp.: emerging global opportunistic pathogens. *Eur J Clin Microbiol Infect Dis* **33:** 291–304.

Santos, M.O.D., Latrive, A., De Castro, P.A.A., De Rossi, W., Zorn, T.M.T., Samad, R.E., *et al*. (2017) Multimodal evaluation of ultra-short laser pulses treatment for skin burn injuries. *Biomed Opt Exp* **8:** 1575–1588.

Shi, C., Wang, C., Liu, H.e., Li, Q., Li, R., Zhang, Y., *et al*. (2020) Selection of appropriate wound dressing for various wounds. *Front Bioeng Biotechnol* **8:** 182.

Shi, H., Xu, X., Zhang, B., Xu, J., Pan, Z., Gong, A., *et al*. (2017) 3,3'-Diindolylmethane stimulates exosomal Wnt11 autocrine signaling in human umbilical cord mesenchymal stem cells to enhance wound healing. *Theranostics* **7:** 1674–1688.

Su, L., Zheng, J., Wang, Y., Zhang, W., and Hu, D. (2019) Emerging progress on the mechanism and technology in wound repair. *Biomed Pharmacother* **117:** 109191.

Thomas-Virnig, C.L., and Allen-Hoffmann, B.L. (2012) A bioengineered human skin tissue for the treatment of infected wounds. *Adv Wound Care (New Rochelle)* **1:** 88–94.

Thönes, S., Rother, S., Wippold, T., Blaszkiewicz, J., Balamurugan, K., Moeller, S., *et al*. (2019) Hyaluronan/collagen hydrogels containing sulfated hyaluronan improve wound healing by sustained release of heparin-binding EGF-like growth factor. *Acta Biomater* **86:** 135–147.

Vågesjö, E., Öhnstedt, E., Mortier, A., Lofton, H., Huss, F., Proost, P., *et al*. (2018) Accelerated wound healing in mice by on-site production and delivery of CXCL12 by transformed lactic acid bacteria. *Proc Natl Acad Sci USA* **115:** 1895–1900.

Williams, N.T. (2010) Probiotics. *Am J Health Syst Pharm* **67:** 449–458.

Wong, D., Nielsen, T.B., Bonomo, R.A., Pantapalangkoor, P., Luna, B., and Spellberg, B. (2017) Clinical and pathophysiological overview of acinetobacter infections: a century of challenges. *Clin Microbiol Rev* **30:** 409–447.

Yoon, D., Yoon, D., Sim, H., Hwang, I., Lee, J.-S., and Chun, W. (2018) Accelerated wound healing by fibroblasts differentiated from human embryonic stem cell-derived mesenchymal stem cells in a pressure ulcer animal model. *Stem Cells Int* **2018:** 4789568.

Zhang, X.G., Li, X.M., Zhou, X.X., Wang, Y., Lai, W.Y., Liu, Y., *et al*. (2019) The wound healing effect of callicarpa nudiflora in scalded rats. *Evid Based Complement Alternat Med* **2019:** 1860680.

Zhou, H.M., Wang, J., Elliott, C., Wen, W., Hamilton, D.W., and Conway, S.J. (2010) Spatiotemporal expression of periostin during skin development and incisional wound healing: lessons for human fibrotic scar formation. *J Cell Commun Signal.* **4:** 99–107.

